

CONFIDENTIAL

290

Copy
RM L52K13

NACA RM L52K13



RESEARCH MEMORANDUM

SMALL-SCALE TRANSONIC INVESTIGATION OF A 45° SWEPTBACK
WING OF ASPECT RATIO 4 WITH COMBINATIONS OF
NOSE-FLAP DEFLECTIONS AND WING TWIST

By William J. Alford, Jr., and Kenneth P. Spreemann

Langley Aeronautical Laboratory
Langley Field, Va.

CLASSIFIED DOCUMENT

This material contains information affecting the National Defense of the United States within the meaning of the espionage laws, Title 18, U.S.C., Secs. 793 and 794, the transmission or revelation of which in any manner to an unauthorized person is prohibited by law.

NATIONAL ADVISORY COMMITTEE
FOR AERONAUTICS

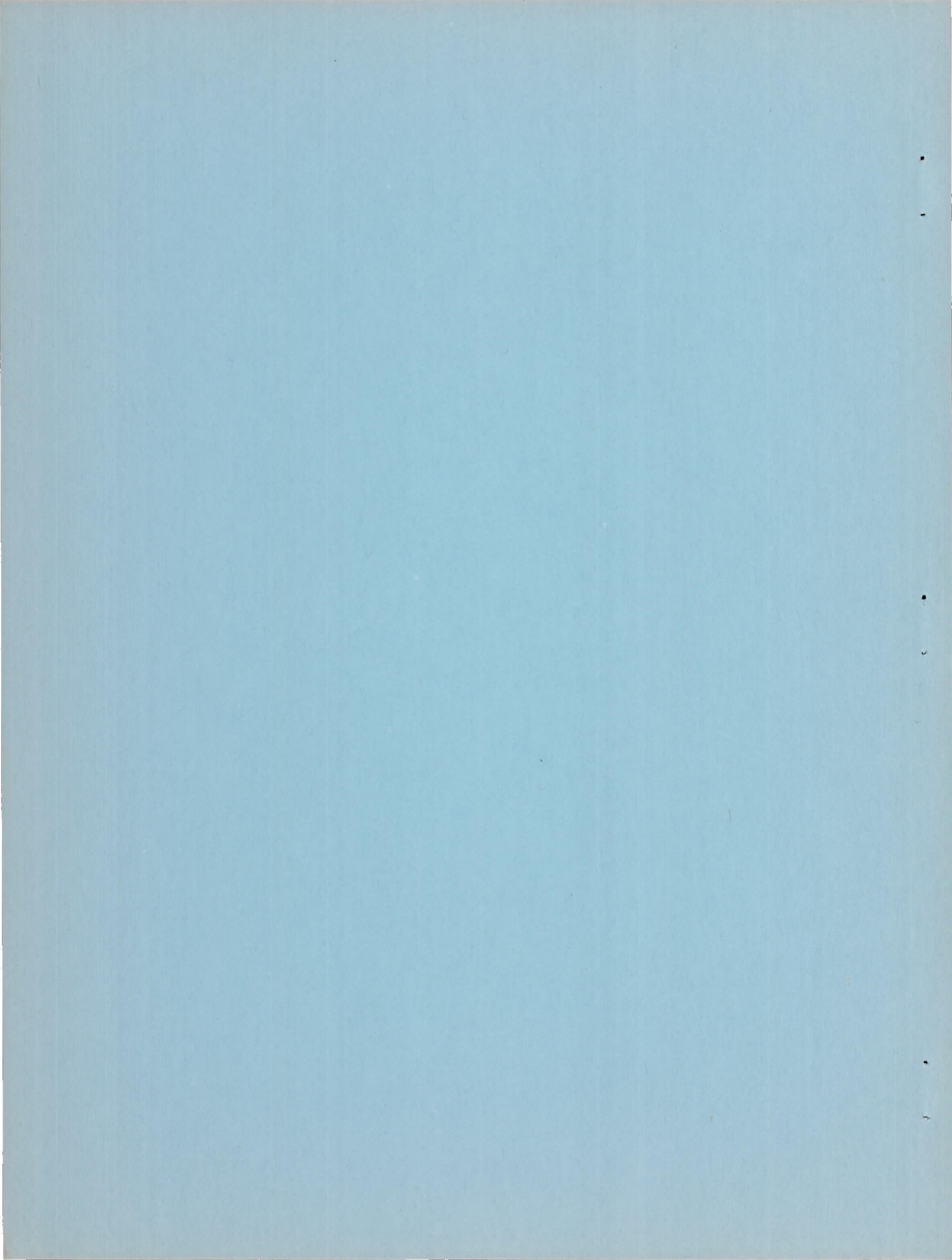
WASHINGTON

January 9, 1953

CLASSIFICATION CHANGED TO UNCLASSIFIED
AUTHORITY: NACA RESEARCH ABSTRACT NO. 109
EFFECTIVE DATE: NOVEMBER 14, 1956

WHL

CONFIDENTIAL



NATIONAL ADVISORY COMMITTEE FOR AERONAUTICS

RESEARCH MEMORANDUM

SMALL-SCALE TRANSONIC INVESTIGATION OF A 45° SWEPTBACK
WING OF ASPECT RATIO 4 WITH COMBINATIONS OF
NOSE-FLAP DEFLECTIONS AND WING TWIST

By William J. Alford, Jr., and Kenneth P. Spreemann

SUMMARY

A small-scale transonic investigation of a semispan wing sweptback 45° and of aspect ratio 4 with combinations of nose-flap deflections and wing twist has been made in the Langley high-speed 7- by 10-foot tunnel over a Mach number range from 0.60 to 1.11. Results are presented of the wing-alone configurations of the basic wing and modifications that consisted of a 6° nose-flap deflection in combination with 0° , 3.3° , and 6.5° washout. Lift, drag, and pitching-moment data were obtained for these configurations.

The results indicated that the maximum lift-drag ratios were improved over those of the basic wing at the lower Mach numbers by the modification consisting of 6° nose-flap deflection and no twist. At the higher Mach numbers the 6° nose flap lost effectiveness, and washout had to be incorporated in order to provide any improvement over the lift-drag characteristics of the basic wing. The variation of the lift-curve slopes, pitching-moment slopes, and minimum drag with Mach number were not greatly affected by the modifications. The angle of attack for zero lift and the pitching moment at zero lift were raised approximately in proportion to the amount of washout incorporated.

INTRODUCTION

Previous investigations at subsonic and transonic speeds (refs. 1 and 2) have shown that the lift-drag ratios of low-aspect-ratio swept-back wings could be substantially improved by the application of wing twist and camber. Inasmuch as twist and camber present several undesirable fabrication problems, an investigation (ref. 3) was made to determine the effectiveness of partial and full-span nose flaps in

improving the lift-drag ratios. The results of this investigation indicated that some improvements were realized from the proper nose-flap configuration up to a Mach number of approximately 0.90, above which the nose-flap effectiveness rapidly decreased.

Unpublished data for a wing identical to the wing of the present investigation, but of larger scale, indicated that a full-span nose-flap configuration with 6° deflection would be about the optimum nose-flap condition from considerations of maximum lift-drag ratios and also verified the results of reference 3 in that the improvements to the lift-drag ratios decreased around a Mach number of 0.90. Twist variations of -3.3° and -6.5° , measured with respect to the root chord, were, therefore, investigated in conjunction with a 6° full-span nose-flap deflection to determine if the beneficial nose-flap characteristics could be extended to higher Mach numbers by unloading the tip sections and providing a more nearly elliptic span load distribution.

The present investigation was made in the Langley high-speed 7-by 10-foot tunnel over a Mach number range from 0.60 to 1.11. Lift, drag, and pitching-moment data were obtained for the various wing-alone configurations.

COEFFICIENTS AND SYMBOLS

C_L lift coefficient, $\frac{\text{Twice semispan lift}}{qS}$

C_D drag coefficient, $\frac{\text{Twice semispan drag}}{qS}$

C_m pitching-moment coefficient referred to $0.25\bar{c}$,
 $\frac{\text{Twice semispan pitching moment}}{qS\bar{c}}$

q effective dynamic pressure over span of model, $\frac{1}{2}\rho V^2$,
 lb/sq ft

S twice wing area of semispan model, 0.125 sq ft

\bar{c} mean aerodynamic chord of wing, based on relationship
 $\frac{2}{S} \int_0^{b/2} c^2 dy$, 0.194 ft

c	local wing chord parallel to plane of symmetry, ft
b	twice span of semispan model, 0.707 ft
y	spanwise distance from plane of symmetry, ft
ρ	air density, slugs/cu ft
V	stream velocity over model, ft/sec
M	effective Mach number, $\frac{2}{S} \int_0^{b/2} c M_a dy$
M_l	local Mach number
M_a	average chordwise Mach number
R	Reynolds number, $\rho V c / \mu$
μ	absolute viscosity, lb-sec/sq ft
α	angle of attack of wing root-chord line, deg
ϵ	angle of wing twist measured relative to wing root-chord plane; negative for washout
δ_η	nose-flap deflection, deg; measured positive down relative to local wing chord (see fig. 1)
$\frac{\partial C_L}{\partial \alpha}$	variation of lift coefficient with angle of attack, per deg; averaged over a lift-coefficient range of ± 0.1
$\frac{\partial C_m}{\partial C_L}$	variation of pitching-moment coefficient with lift coefficient; averaged over a lift-coefficient range of ± 0.1
$\alpha_{C_L=0}$	angle of attack for zero lift coefficient, deg
C_{m_0}	pitching-moment coefficient at zero lift coefficient
$C_{D_{min}}$	minimum drag coefficient
$C_{L_{D_{min}}}$	lift coefficient at minimum drag coefficient

L/D lift-drag ratio

$(L/D)_{\max}$ maximum lift-drag ratio

$\frac{(L/D)_{\max \delta_n=6^\circ, \epsilon}}{(L/D)_{\max \delta_n=0^\circ, \epsilon=0^\circ}}$ performance ratio: maximum lift-drag ratio of wing with nose flap deflected 6° and with varying twist angle ϵ referred to the maximum lift-drag ratio of the basic wing

$C_L(L/D)_{\max}$ lift coefficient at maximum lift-drag ratio

MODEL AND APPARATUS

The beryllium-copper wing employed in this investigation had 45° sweepback referred to the quarter-chord line with aspect ratio 4, taper ratio 0.3, and NACA 65A006 airfoil section parallel to the free stream. A drawing of the model, including the full-span deflection, is shown in figure 1. A photograph of the model mounted on the reflection plane is shown in figure 2.

The basic wing ($\delta_n = 0^\circ$, $\epsilon = 0^\circ$) was modified by cutting in the lower surface of the wing along the 20-percent streamwise chord a spanwise groove about $1/32$ inch wide and about half the depth of the local section. The root chord was cut back to the $0.20c$ station. The alterations were performed previous to testing and were filled with solder for the basic-wing configuration. The flap angle was obtained by bending the leading-edge segment of the wing about the 0.20 -chord line. After setting the flap angle, the groove was filled and made flush with the wing surface. Angular distortion of the flap under load was negligible. Twist variations (fig. 3), corresponding to twist angles of -3.3° and -6.5° at the wing tip, were obtained by physically twisting the basic wing at several spanwise stations.

Force and moment measurements were made with a strain-gage balance system and recorded with recording potentiometers. The angle of attack was measured by a slide-wire potentiometer.

TESTS

The investigation was made in the Langley high-speed 7- by 10-foot tunnel with the model mounted on a reflection plane (fig. 1) located

approximately 3 inches from the tunnel wall in order to bypass the wall boundary layer. The reflection-plane boundary-layer thickness was such that a value of 95 percent of free-stream velocity was reached at a distance of approximately 0.16 inch from the surface of the reflection plane for all test Mach numbers. This boundary-layer thickness represented a distance of about 4 percent semispan for the model tested.

At Mach numbers below 0.93, there was practically no velocity gradient in the vicinity of the reflection plane. At higher Mach numbers, however, the presence of the reflection plane created a high local-velocity field which permitted testing the models up to $M = 1.11$ before choking occurred in the tunnel. The variations of local Mach numbers in the region occupied by the model are shown in figure 4. Effective test Mach numbers were obtained from contour charts similar to those shown in figure 4 from surveys made with no model in position by the relationship

$$M = \frac{2}{S} \int_0^{b/2} c M_a dy$$

For the models tested, Mach number variations (outside the boundary layer) of less than 0.01 were obtained generally below $M = 0.95$. Local Mach number variations from about 0.05 to 0.07 were obtained in a range from $M = 0.98$ to $M = 1.11$. It should be noted that the Mach number gradient is principally chordwise.

A gap of about $1/16$ inch was maintained between the wing root-chord section and the reflection-plane turntable. A sponge-wiper seal was fastened to the wing butt behind the turntable to minimize leakage. Force and moment measurements were made for the model over a Mach number range from 0.60 to 1.11 and an angle-of-attack range from -6° to 22° . The variation of Reynolds number with Mach number for these tests is shown in figure 5.

In view of the small size of the model in relation to the tunnel test section, jet-boundary and blockage corrections were believed to be negligible and were not applied to these data. Cutting the root chord back to the $0.20c$ station and grooving the lower surface of the wing to facilitate deflecting the nose flap increased the aeroelastic twist only slightly over the comparatively small twist as reported in reference 4. In view of the small corrections resulting from this twist, no aeroelastic corrections were applied to these data.

In general, the accuracy of the force and moment measurements can be judged by any random scatter of the test points used in presenting the basic data. In applying a technique that utilizes small reflection-plane models mounted in a localized high-velocity field, the reliability of the absolute values of some of the results, particularly the drag

values, may be open to question. Experience has indicated, however, that valid determinations of incremental effects, such as those due to lift coefficient, Mach number, or changes in model configuration, normally can be obtained. A more complete evaluation of results obtained by techniques such as that used for the present investigation is given in reference 5.

RESULTS AND DISCUSSION

The basic-wing data for the test configurations are presented in figure 6 and the lift-drag ratios are presented in figure 7. The performance ratios and the summary of aerodynamic characteristics of the test model are presented in figures 8 and 9, respectively. The lift-curve and pitching-moment slopes presented herein have been averaged over a lift-coefficient range of ± 0.1 . It may be noted that quantitative differences of approximately 15 to 20 percent in lift-curve slopes and of approximately 5 to 7 percent mean aerodynamic chord in aerodynamic-center locations exist between the basic-wing data of the present paper and the basic-wing data of reference 4. The reasons for these differences are unaccounted for; however, it is felt that the incremental effects of the various modifications incorporated in the basic wing for this investigation are valid. This belief is based on the general similarity between the incremental effects of this paper and those reported in reference 3, and also those evident in unpublished data on a similar wing of larger scale.

Lift Characteristics

In general, the trends with Mach number of the lift-curve slopes $\partial C_L / \partial \alpha$ were not greatly affected by any of the modifications tested (fig. 9). However, the configuration employing -6.5° twist and 6° nose flaps indicated the greatest reductions throughout the Mach number range investigated (about 0.005).

Inspection of the values of the angle of attack for zero lift $\alpha_{C_L=0}$ indicates that Mach number had small effect on this parameter. Deflection of the nose flap 6° downward caused the value of $\alpha_{C_L=0}$ to become slightly positive (about 0.2°). Varying the twist from $\epsilon = 0^\circ$ to $\epsilon = -3.3^\circ$ in conjunction with the 6° nose flap caused the value of $\alpha_{C_L=0}$ to increase substantially (2.5°). Further variation of the twist to $\epsilon = -6.5^\circ$ caused $\alpha_{C_L=0}$ to increase to approximately twice the value obtained for $\epsilon = -3.3^\circ$. It should be noted that the rather

large change in $\alpha_{C_L=0}$ due to twist resulted primarily from the wing being twisted relative to the root-chord line, which served as the angle-of-attack reference line.

Drag Characteristics

The effect of the modifications was to increase the minimum drag $C_{D_{min}}$ slightly and this increase remained relatively constant throughout the Mach number range tested (fig. 9). The drag-break Mach number $\frac{\partial C_D}{\partial M} = 0.1$ of the basic wing was 0.98 and was practically unaffected by any of the modifications.

The values of the lift coefficient for minimum drag $C_{L_{C_{D_{min}}}}$ indicate that the modifications caused $C_{D_{min}}$ to occur at somewhat higher lift coefficients than for the basic wing. The variations of $C_{L_{C_{D_{min}}}}$ with Mach number were found to be small for all configurations tested.

Lift-Drag Ratios

The absolute values of the lift-drag ratios for the various configurations are presented in figure 7. Inasmuch as the values of $C_{D_{min}}$ may be somewhat high, as previously pointed out in the discussion of the accuracy of force and moment measurements, it is felt that a more reliable basis for evaluating the effects of nose flaps and wing twist on the performance characteristics can be obtained by defining a performance ratio as the following:

$$\frac{(L/D)_{\max \delta_\eta=0^\circ, \epsilon}}{(L/D)_{\max \delta_\eta=0^\circ, \epsilon=0^\circ}}$$

The variation of the performance ratio as a function of the wing twist angle ϵ is presented in figure 8 and as a function of Mach number in figure 9. In figure 9 it is seen that at the lowest Mach numbers the 6° nose flaps with no twist produced the greatest improvement in $(L/D)_{\max}$ (approx. 23 percent) over the basic wing. At the higher Mach numbers, however, the 6° nose flap lost effectiveness, and washout had to be incorporated in order to provide any improvement over the characteristics of the basic wing. A gain of approximately 15 percent was provided by -6.5° twist with 6° nose flaps at $M = 1.11$.

The effects of the modifications on the lift coefficient for $(L/D)_{\max}$ (fig. 9) were to cause higher values of $C_{L(L/D)_{\max}}$ than those for the basic wing, with little variation due to Mach number up to Mach numbers from 0.95 to 1.00. Above Mach numbers from 0.95 to 1.0 a somewhat sharper rise in $C_{L(L/D)_{\max}}$ with Mach number resulted from incorporation of each of the modifications.

Pitching-Moment Characteristics

Comparison of the pitching-moment slopes $\partial C_m / \partial C_L$ (fig. 9) indicates that the effect of the modifications was to move the aerodynamic-center location an average of approximately 4 percent forward of that of the basic wing below a Mach number of 0.93. At higher Mach numbers the aerodynamic-center locations of the modified configurations moved rearward and were approximately the same as those of the basic wing.

The values of the pitching-moment coefficient at zero lift C_{m_0} for all modifications indicated, in general, a slight positive increase with increasing Mach number. For the 6° nose-flap modification without twist, C_{m_0} was slightly negative and increased positively as the washout was increased.

An inspection of figure 6(c) indicates that neither the nose flaps alone nor the nose flaps in combination with wing twist greatly affected the longitudinal instability at the higher lift coefficients, but, in some instances, these modifications resulted in a slight increase in the lift coefficient at which the instability occurred.

CONCLUSIONS

A small-scale transonic investigation of a semispan wing swept back 45° and of aspect ratio 4 with combinations of nose-flap deflections and wing twist indicated the following conclusions:

1. The maximum lift-drag ratios were improved over those of the basic wing at the lowest Mach numbers by the modification consisting of 6° nose-flap deflection and no twist. At the higher Mach numbers, however, the 6° nose flap lost effectiveness, and washout had to be incorporated in order to provide any improvement over the lift-drag characteristics of the basic wing.

2. The trends with Mach number of the lift-curve slopes and the minimum drag were not greatly affected by any of the modifications. The angle of attack for zero lift was only slightly affected by the 6° nose flap; however, washout in combination with the 6° nose flap increased the values of the angle of attack for zero lift coefficient in proportion to the amount of washout.

3. The pitching-moment slopes were not greatly affected by any of the modifications; however, the pitching-moment coefficient at zero lift coefficient for the 6° nose-flap modification without twist was negative and increased positively as the washout was increased. The incorporation of the various modifications did not greatly affect the longitudinal instability at the higher lift coefficients, but in some instances these modifications resulted in a slight increase in the lift coefficient at which the instability occurred.

Langley Aeronautical Laboratory,
National Advisory Committee for Aeronautics,
Langley Field, Va.

REFERENCES

1. Spreemann, Kenneth P., and Alford, William J., Jr.: Investigation of the Effects of Twist and Camber on the Aerodynamic Characteristics of a $50^{\circ}38'$ Sweptback Wing of Aspect Ratio 2.98. Transonic-Bump Method. NACA RM L51C16, 1951.
2. Jones, J. Lloyd, and Demele, Fred A.: Aerodynamic Study of a Wing-Fuselage Combination Employing a Wing Swept Back 63° .- Characteristics Throughout the Subsonic Speed Range With the Wing Cambered and Twisted for a Uniform Load at a Lift Coefficient of 0.25. NACA RM A9D25, 1949.
3. Spreemann, Kenneth P., and Alford, William J., Jr.: Small-Scale Transonic Investigation of the Effects of Full-Span and Partial-Span Leading-Edge Flaps on the Aerodynamic Characteristics of a $50^{\circ}38'$ Sweptback Wing of Aspect Ratio 2.98. NACA RM L52E12, 1952.
4. Spreemann, Kenneth P. and Alford, William J., Jr.: Small-Scale Investigation at Transonic Speeds of the Effects of Thickening the Inboard Section of a 45° Sweptback Wing of Aspect Ratio 4, Taper Ratio 0.3, and NACA 65A006 Airfoil Section. NACA RM L51F08a, 1951.
5. Donlan, Charles J., Myers, Boyd C., II, and Mattson, Axel T.: A Comparison of the Aerodynamic Characteristics at Transonic Speeds of Four Wing-Fuselage Configurations as Determined From Different Test Techniques. NACA RM L50H02, 1950.

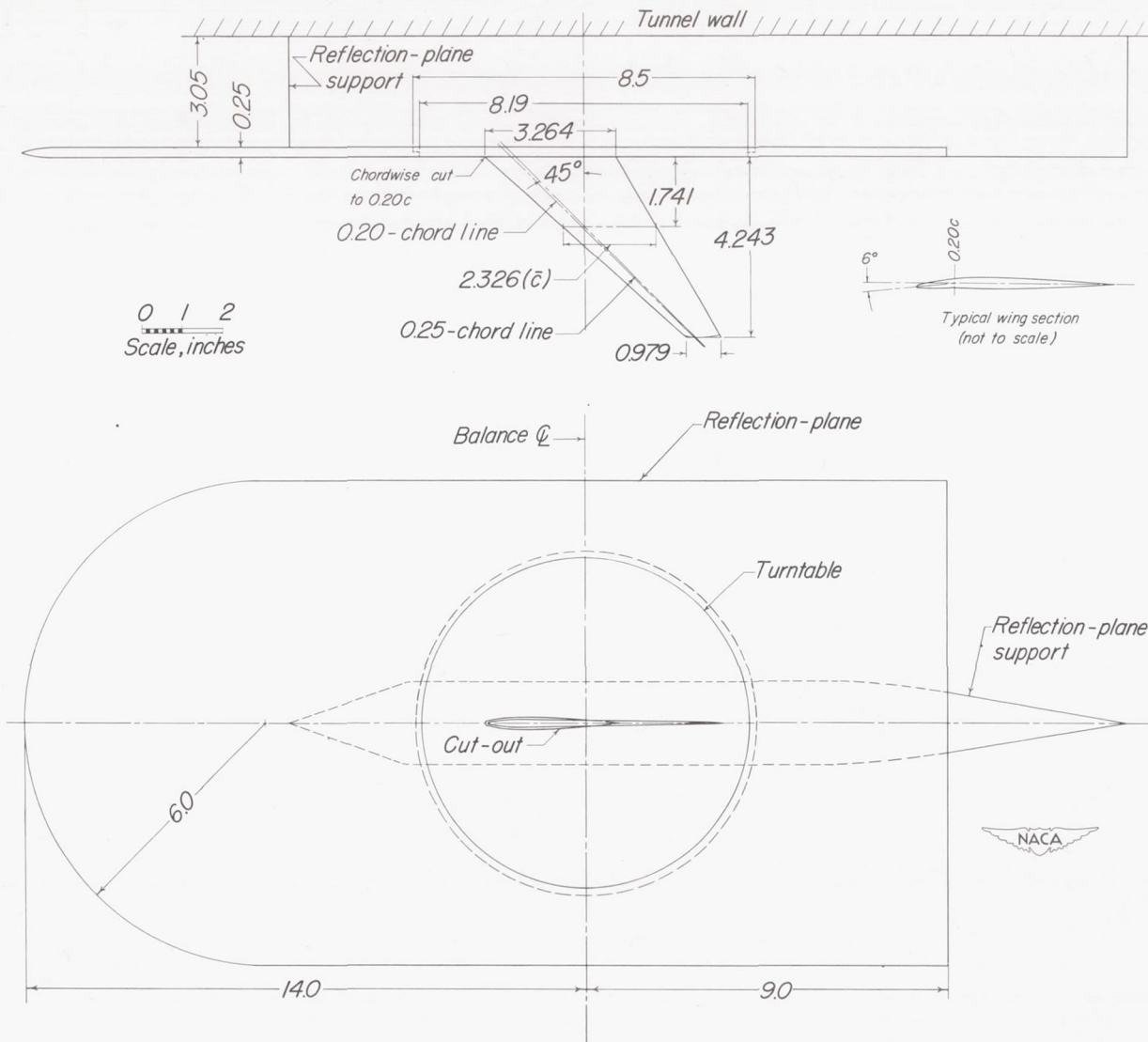


Figure 1.- Two-view drawing of test model mounted on reflection plane.

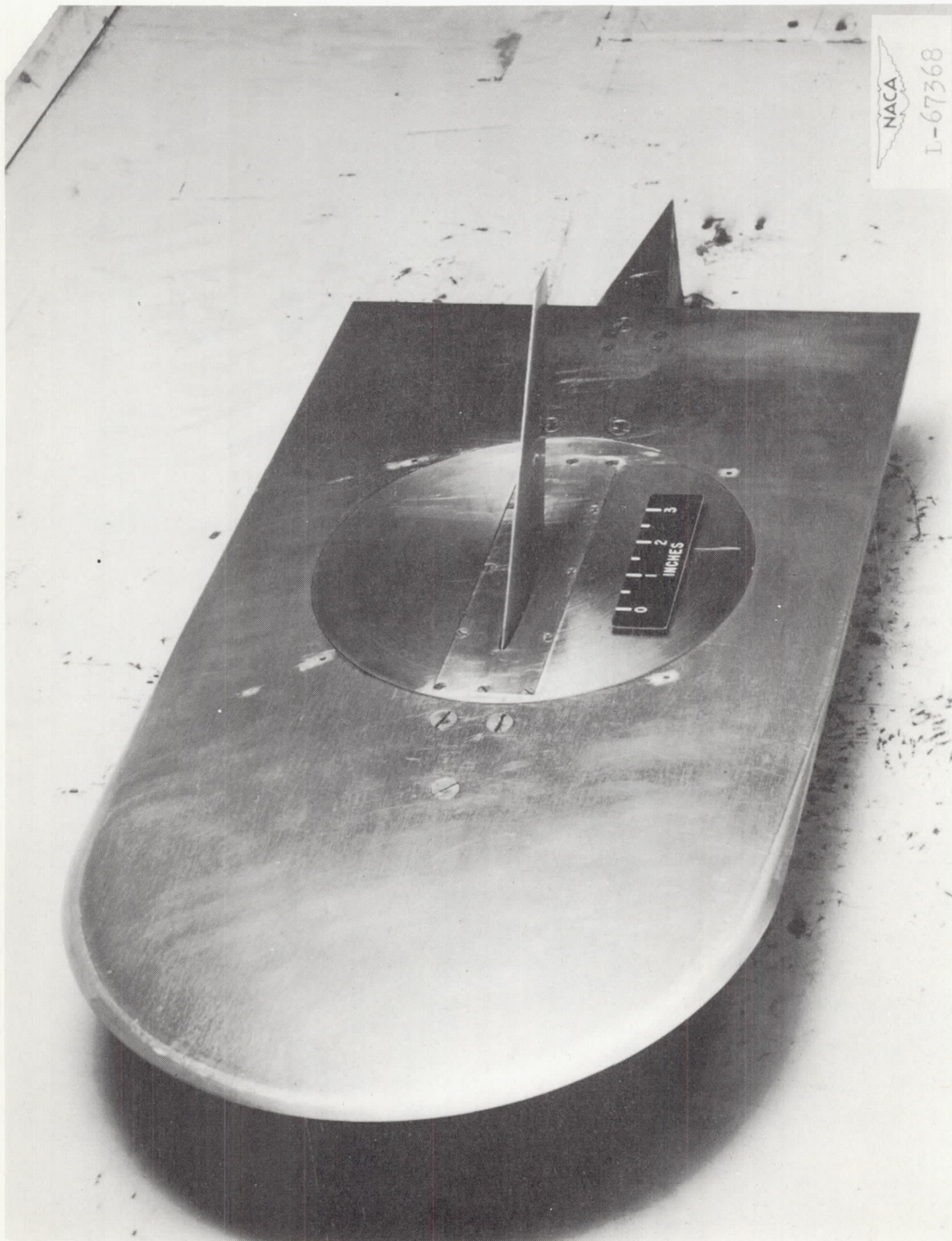


Figure 2.- Photograph of test model on reflection plane.

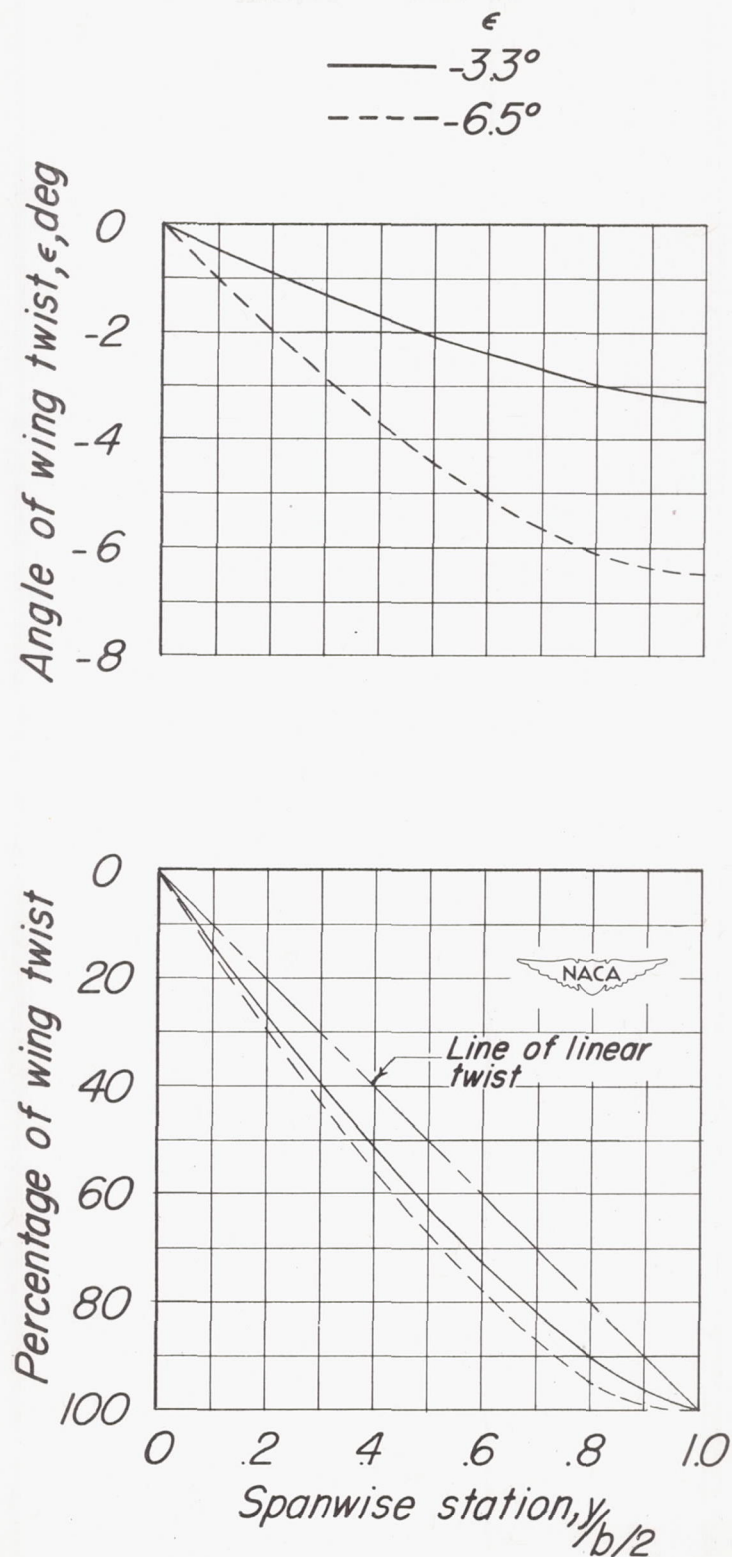
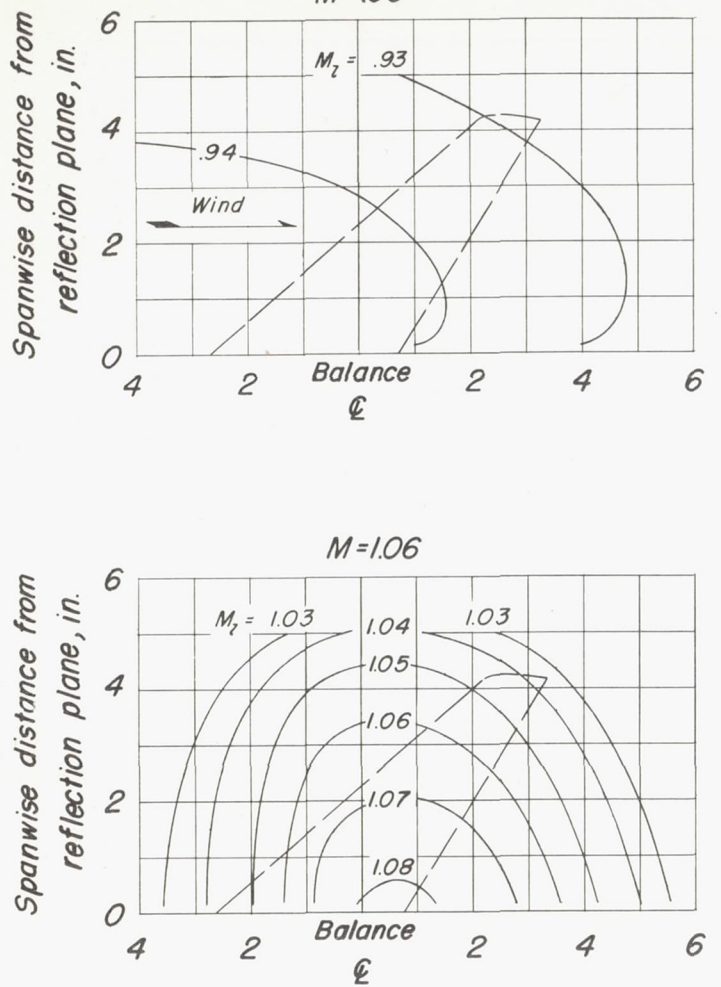
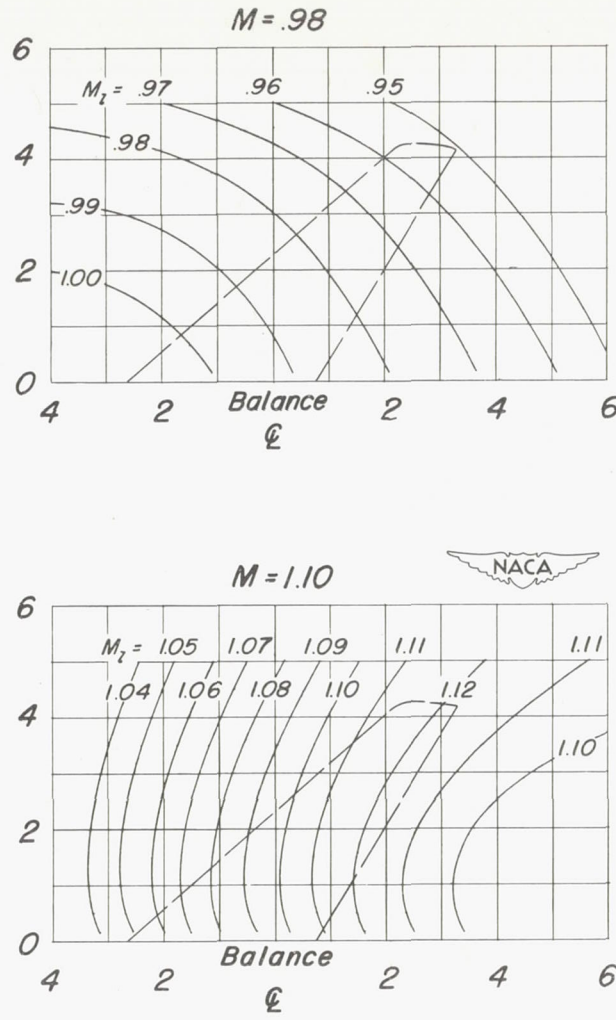


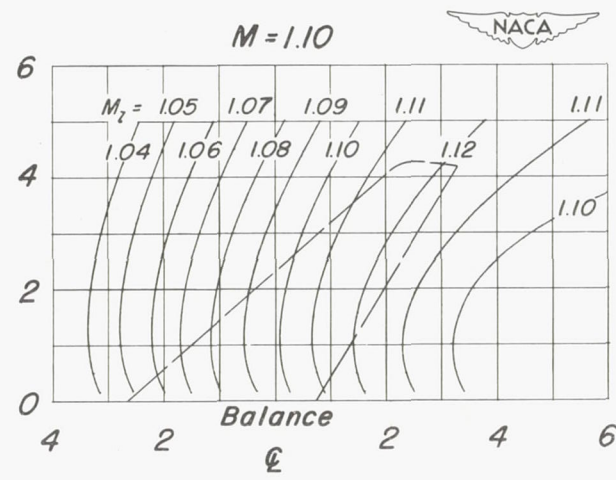
Figure 3.- Spanwise variation of twist of the test model.



Longitudinal distance along reflection plane, in.



Longitudinal distance along reflection plane, in.



NACA RM 152K13

Figure 4.- Typical Mach number contour over reflection plane in region of model location.

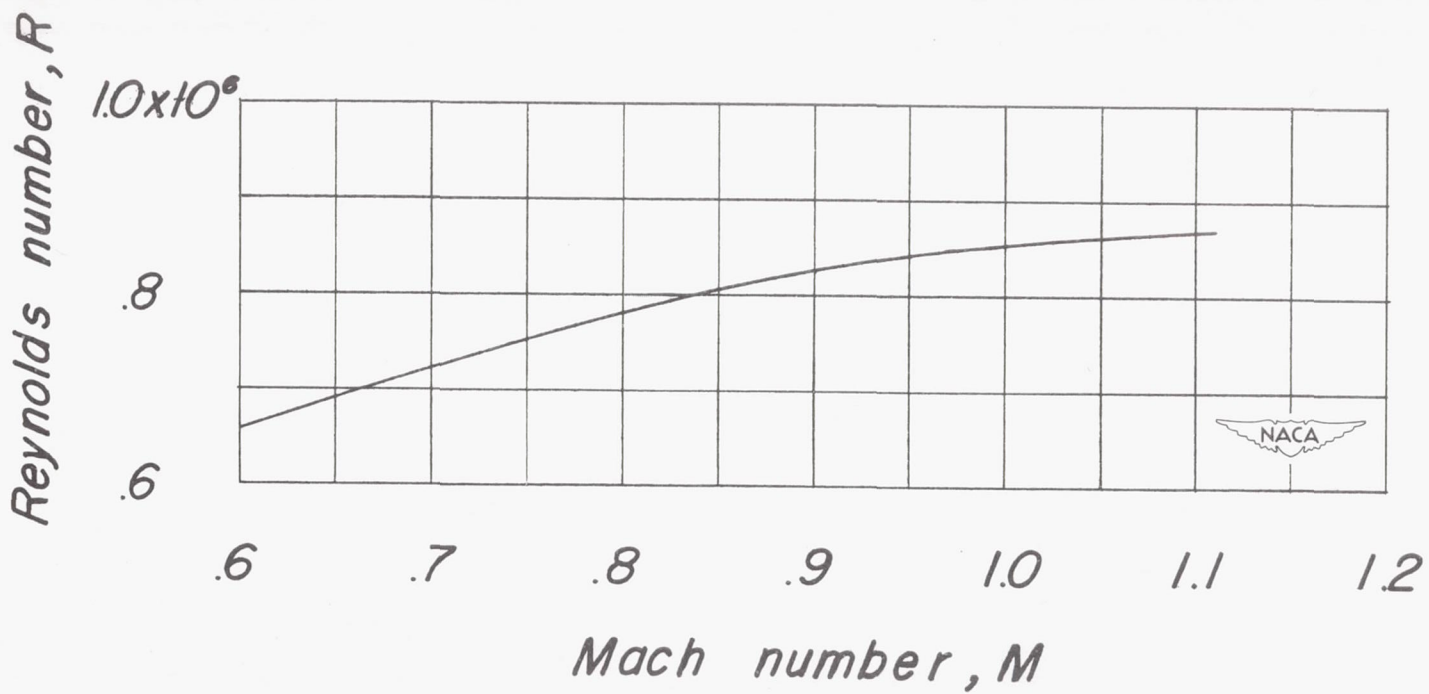


Figure 5.- Variation of Reynolds number with Mach number for the test model.

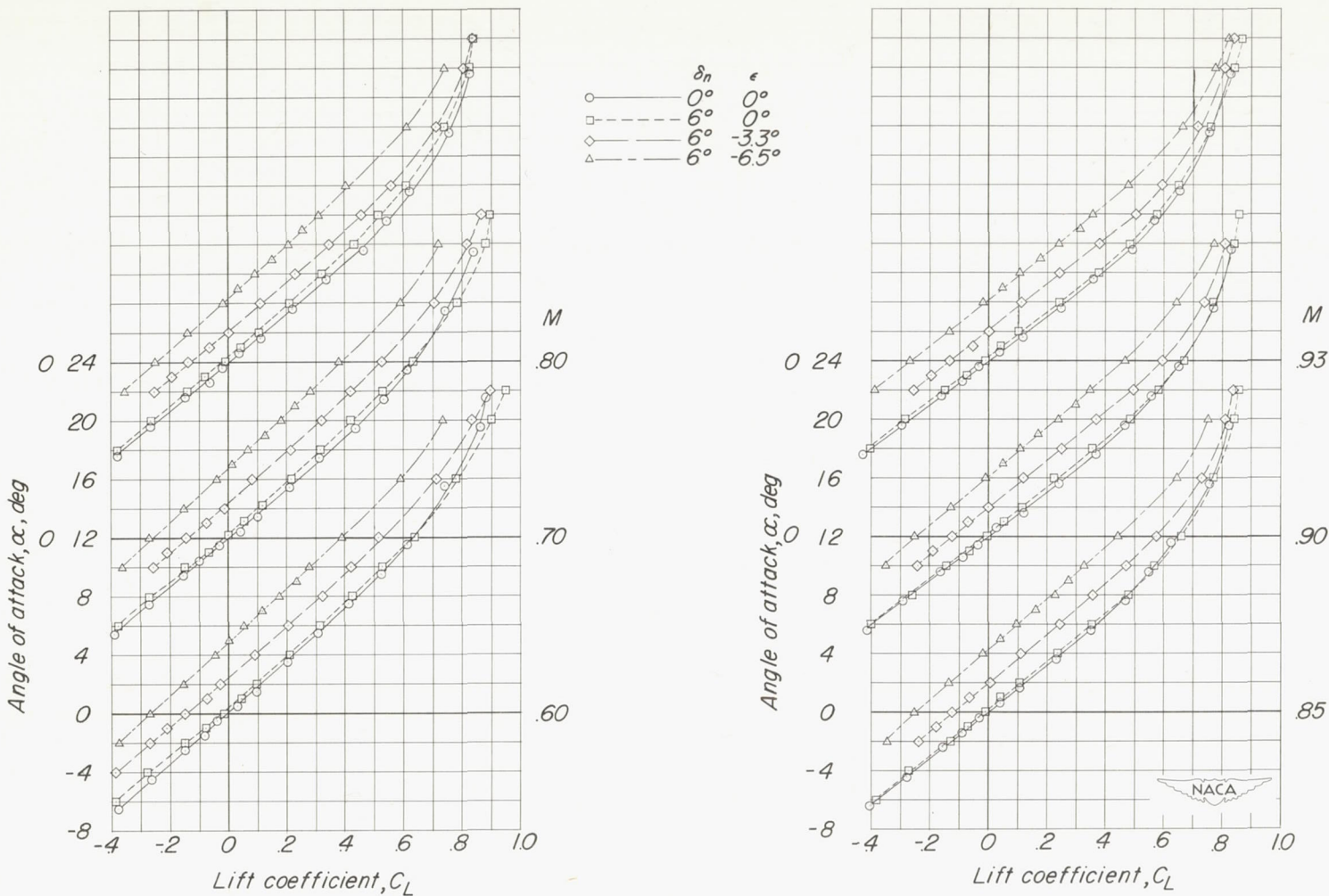
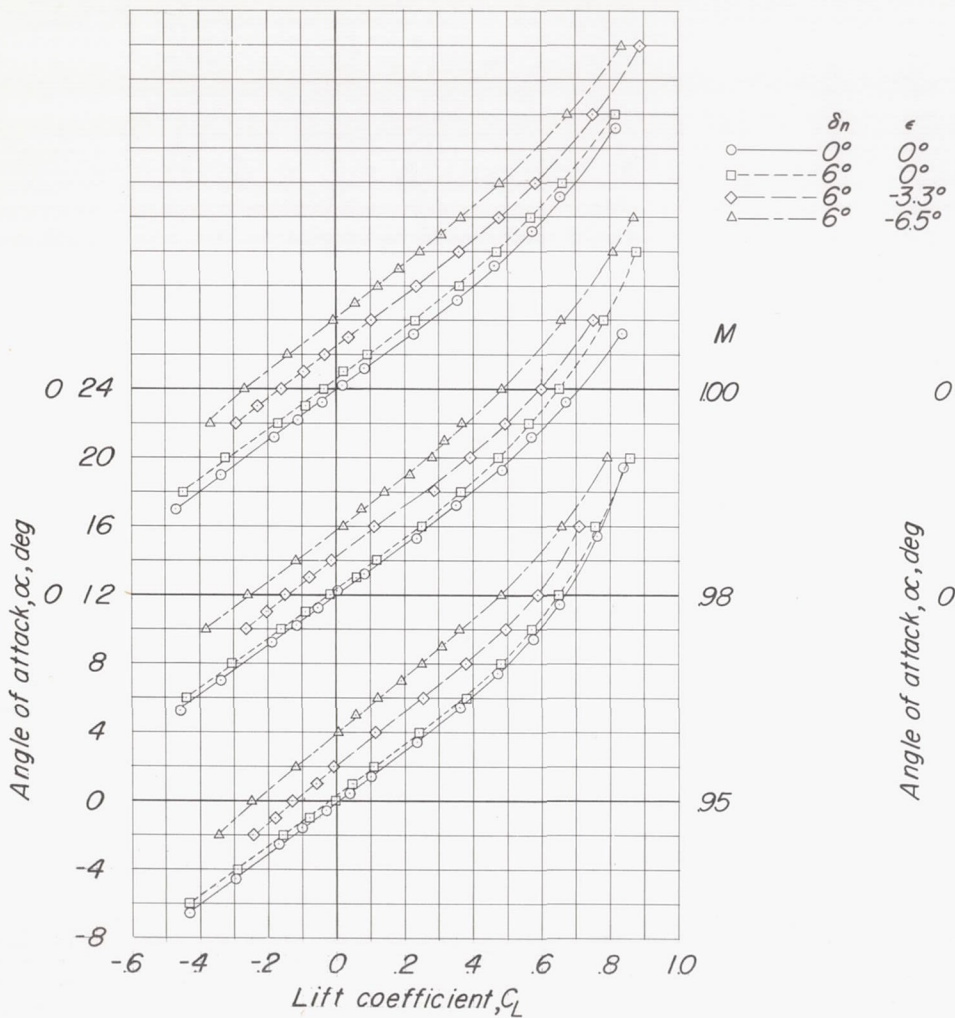
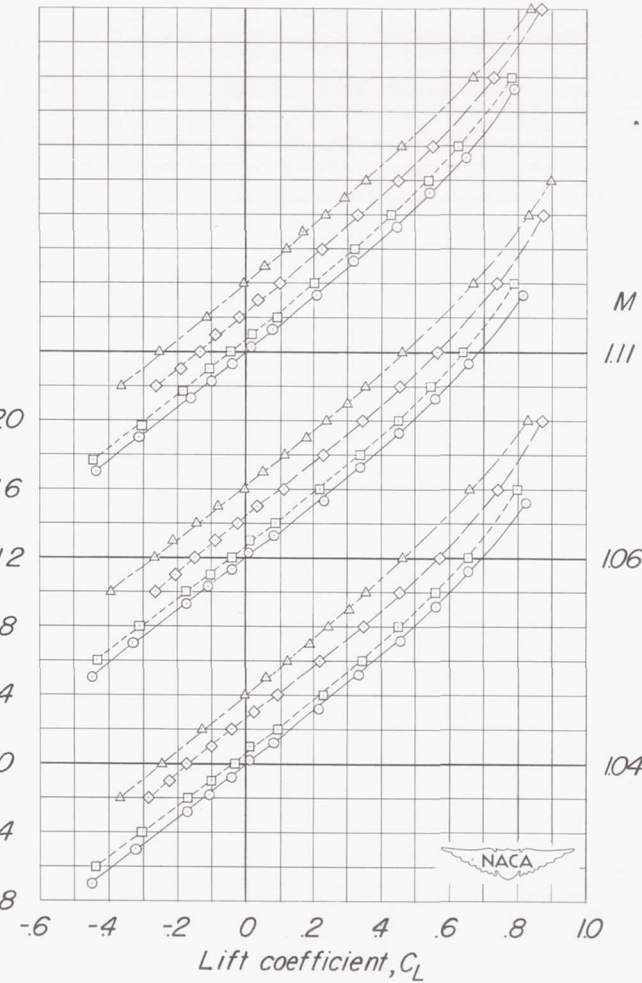
(a) α against C_L .

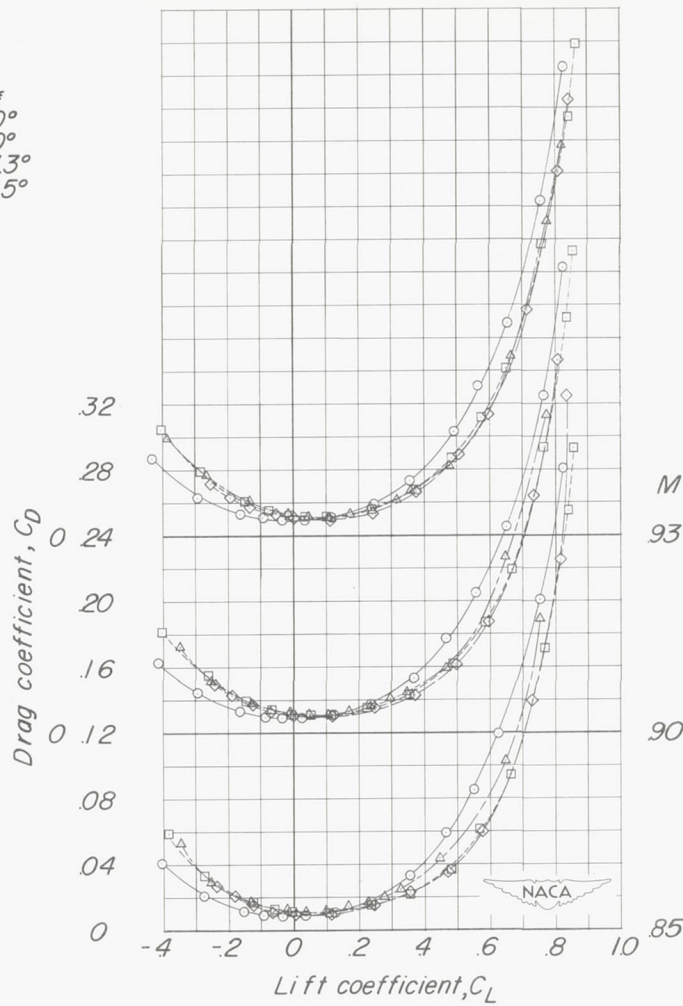
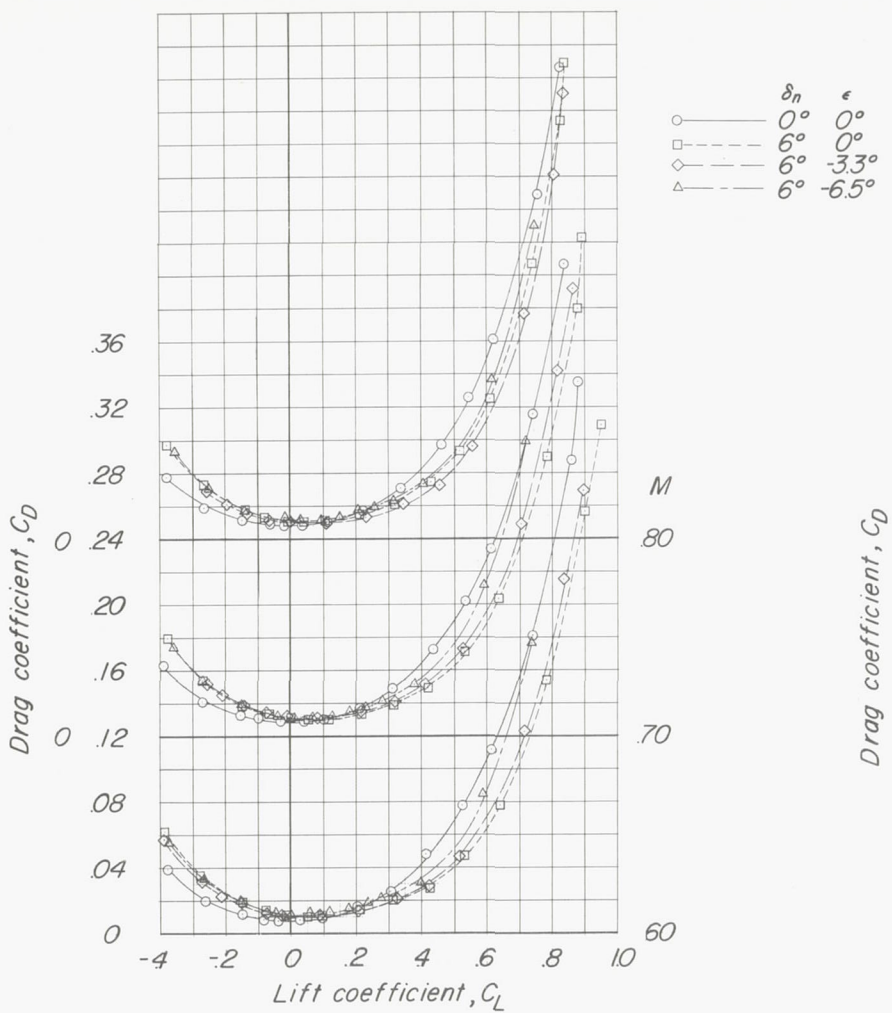
Figure 6.- Aerodynamic characteristics of the test model.



(a) Concluded.

Figure 6.- Continued.

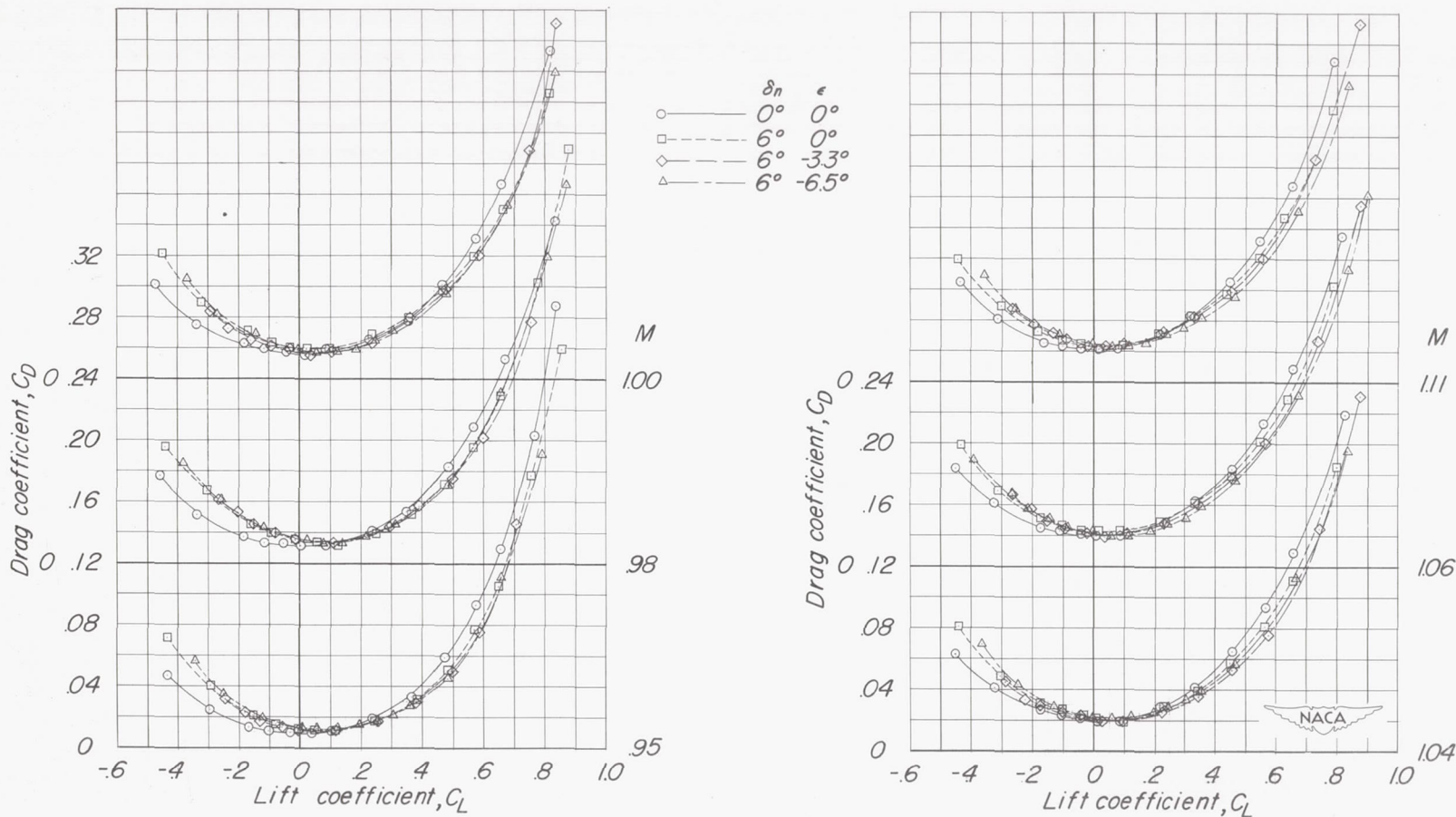




(b) C_D against C_L .

Figure 6.- Continued.

CONFIDENTIAL



(b) Concluded.

Figure 6.- Continued.

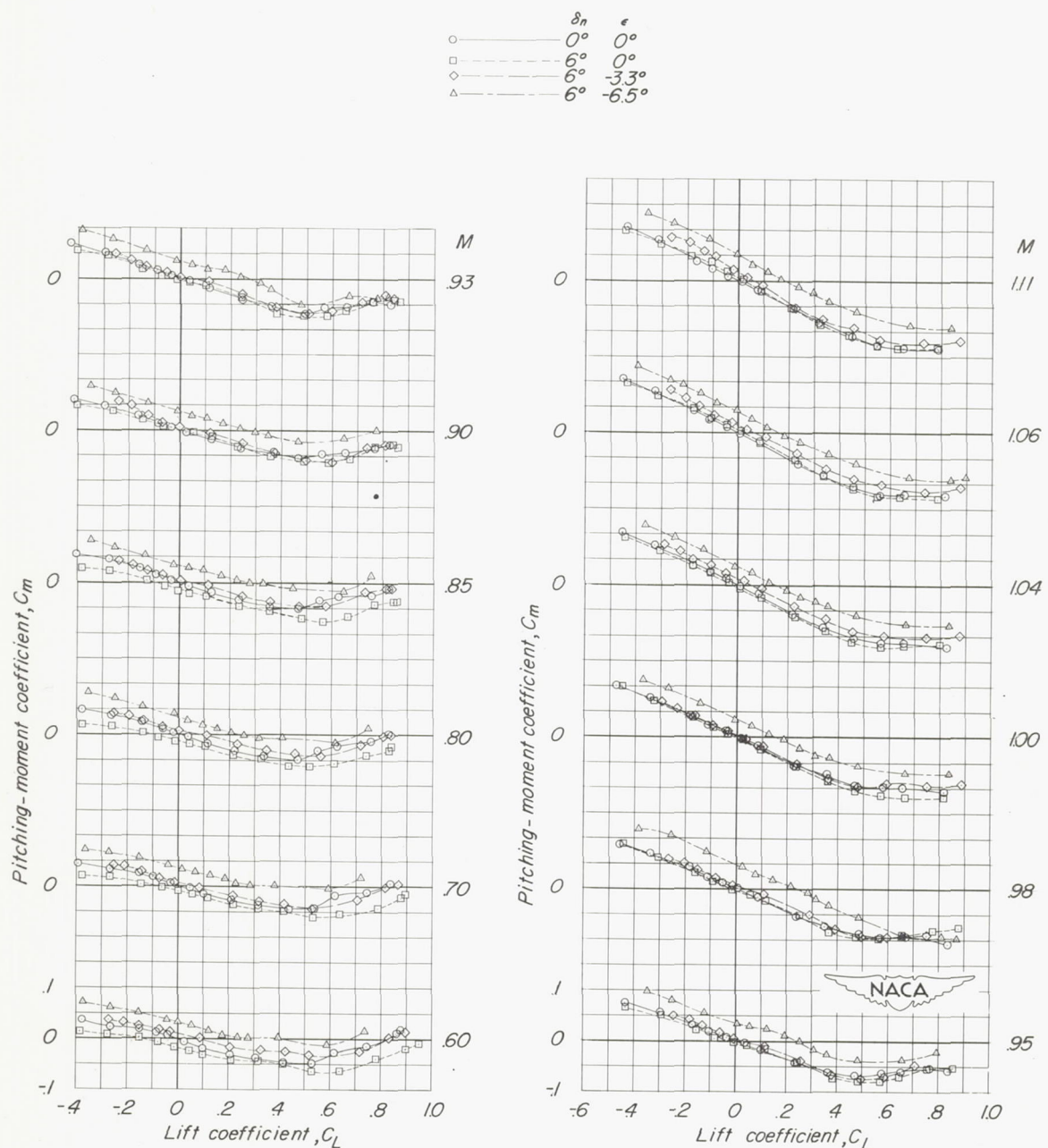
(c) C_m against C_L .

Figure 6.- Concluded.

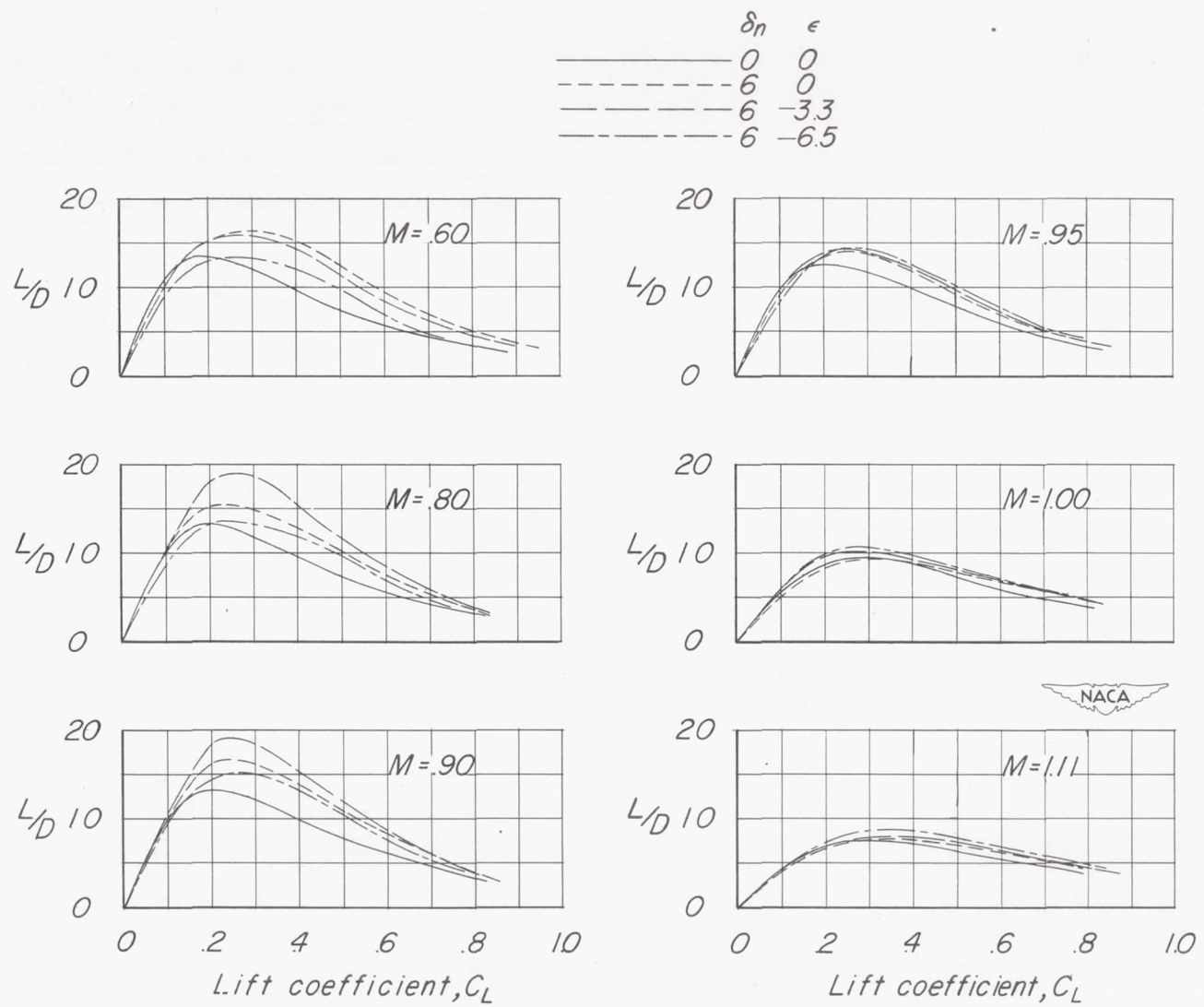


Figure 7.- Lift-drag ratios of the test model.

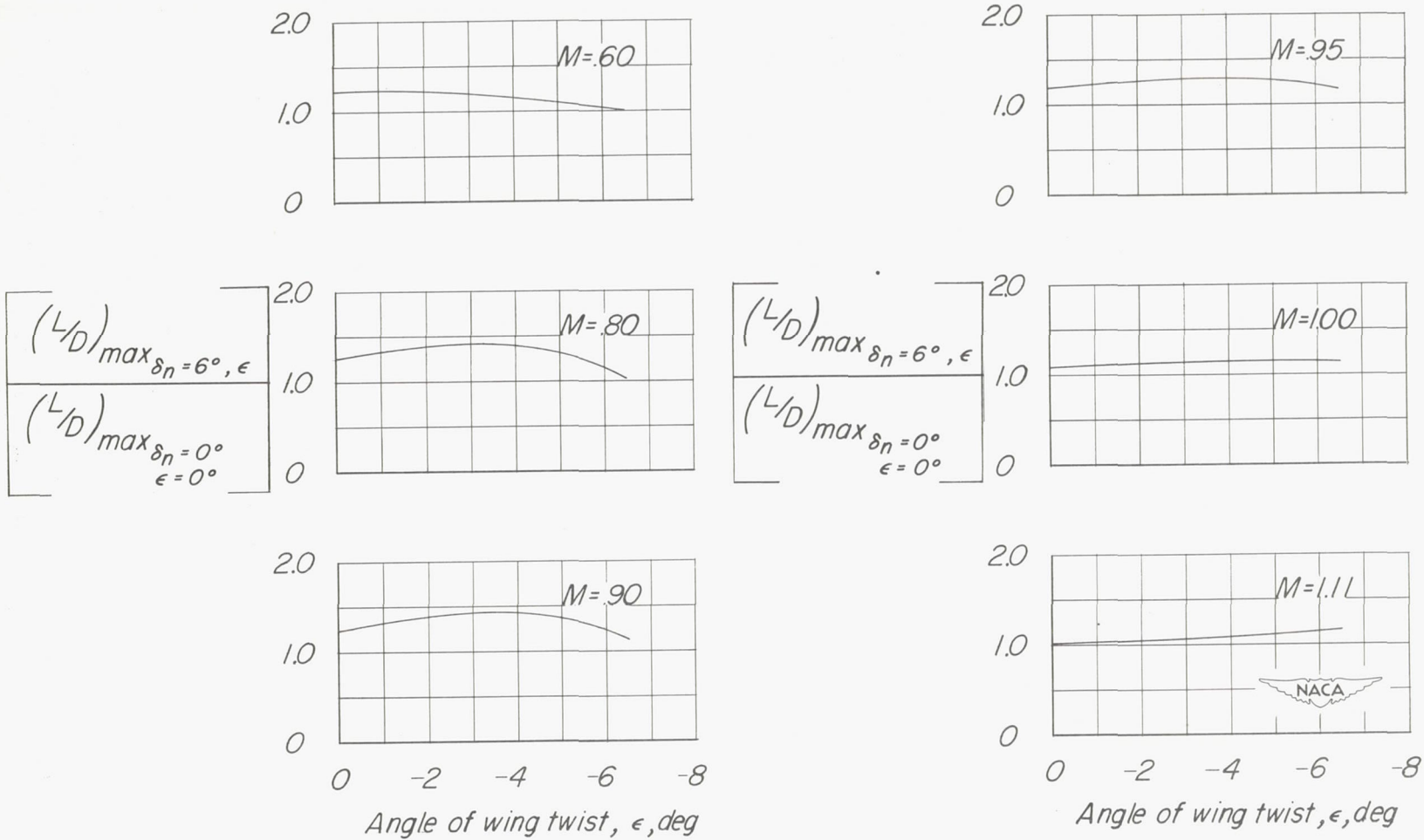


Figure 8.- Performance ratios of the test model.

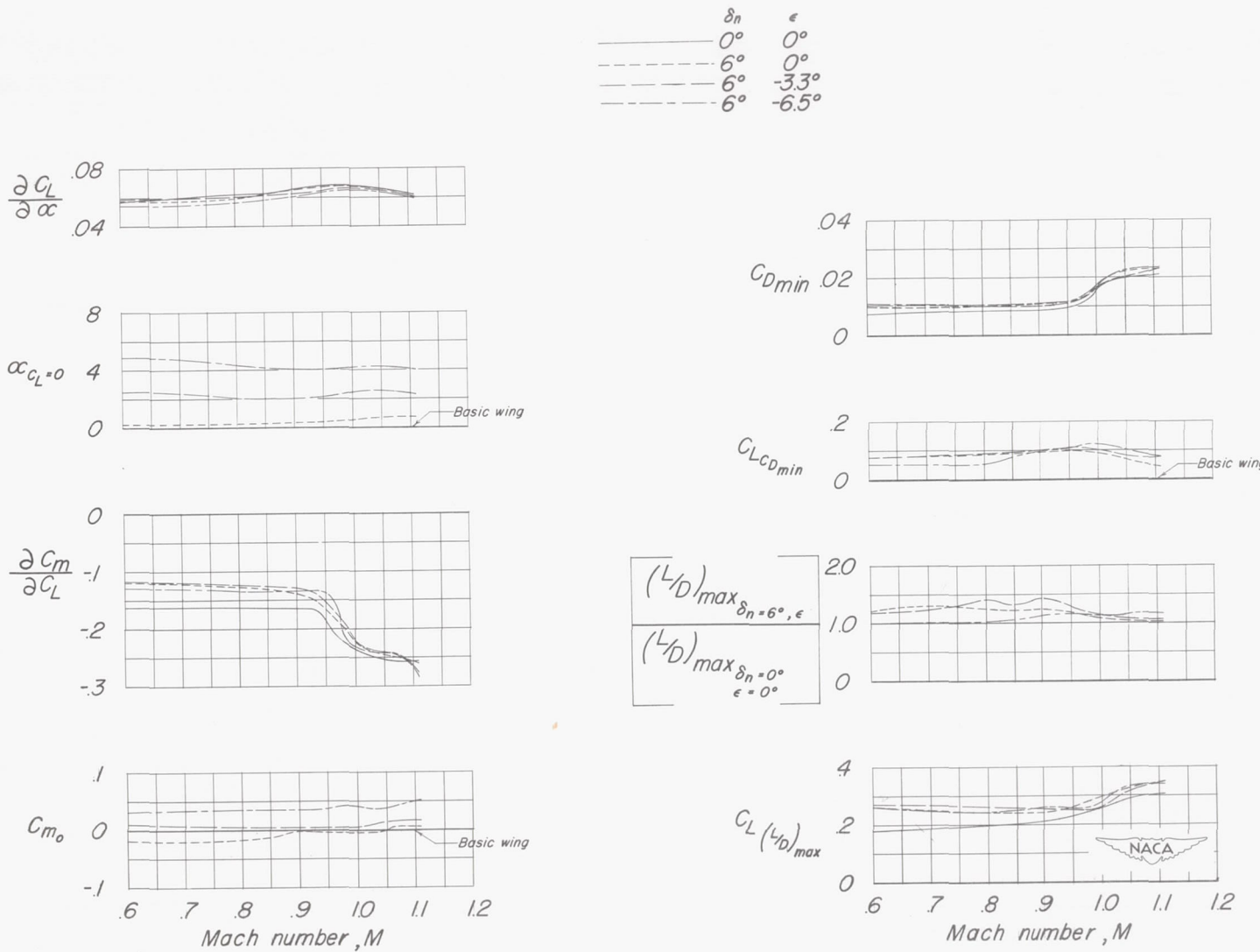
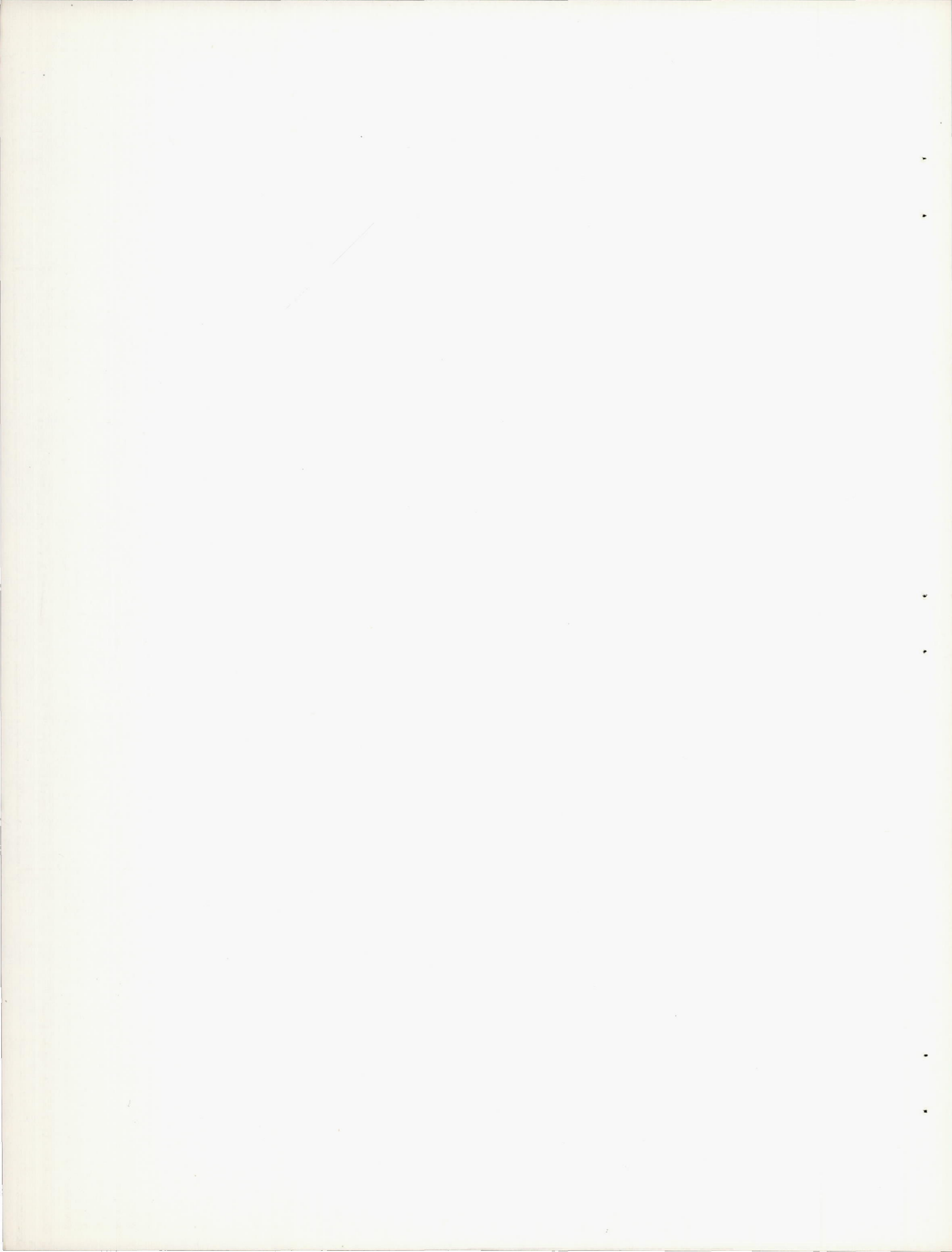
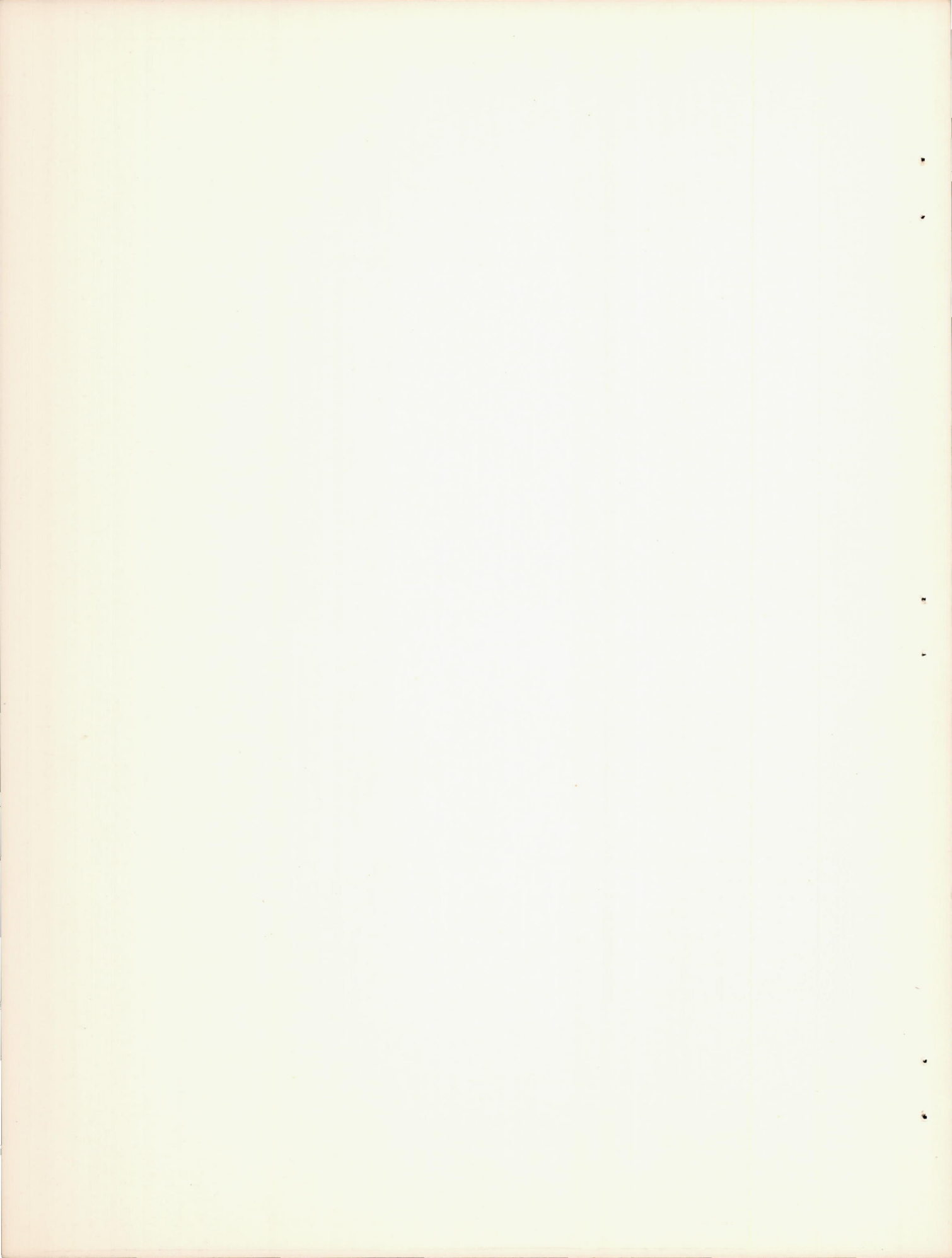
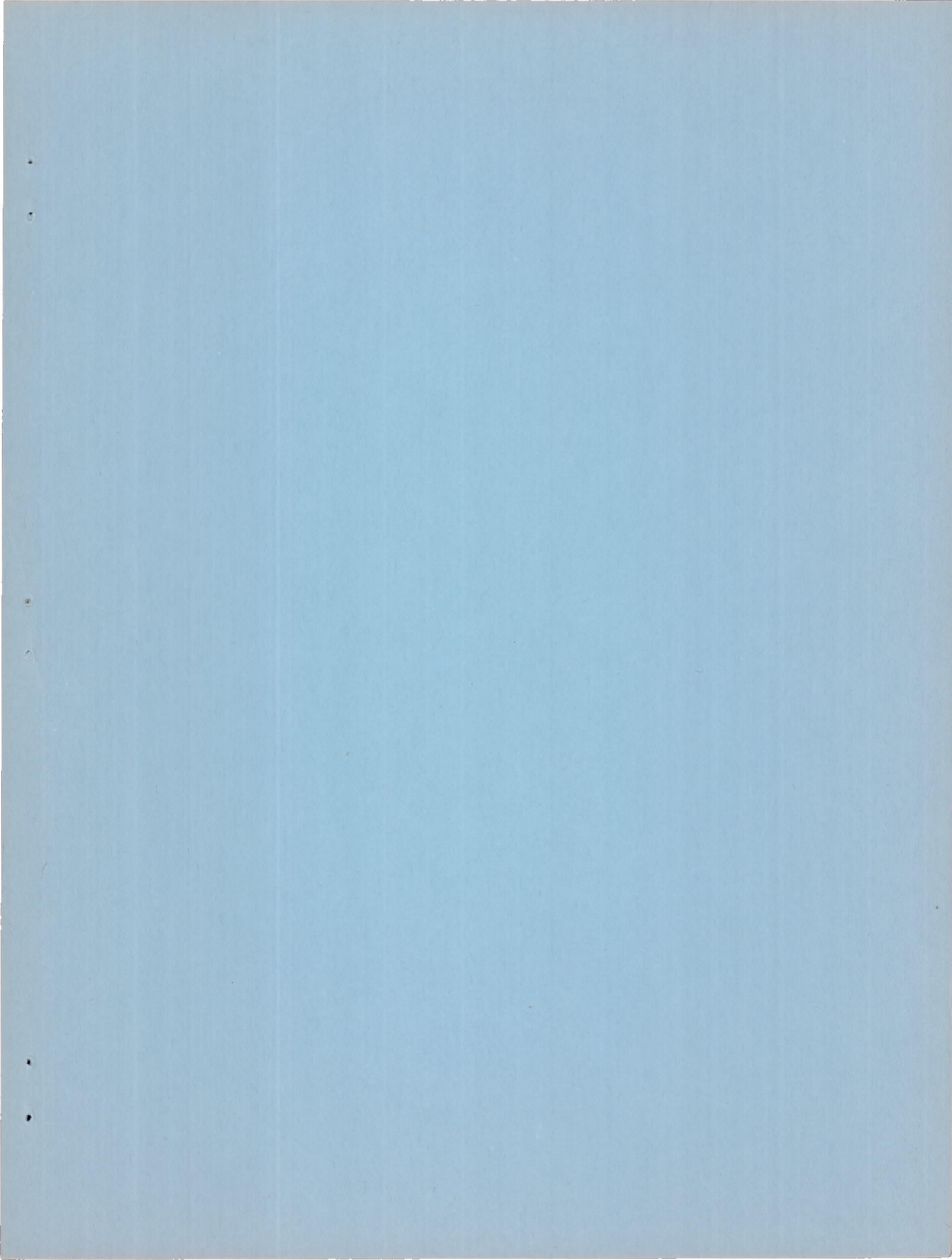


Figure 9.- Summary of aerodynamic characteristics of the test model.







SECURITY INFORMATION

CONFIDENTIAL

CONFIDENTIAL